Skeletal Radiol (1994) 23:327–332

Skeletal Radiology

Articles

Benign soft tissue masses of the wrist and hand: MRI appearances

Theodore T. Miller, M.D.[1], Hollis G. Potter, M.D.[1], Richard R. McCormack, Jr., M.D. [2]

[1] Departments of Radiology and Nuclear Medicine, The Hospital for Special Surgery, Cornell University Medical College, New York, New York, USA
[2] Department of Orthopedic Surgery, The Hospital for Special Surgery, Cornell University Medical College, New York, New York, USA

Abstract. We reviewed 20 cases of soft tissue masses of the hand and wrist, and compared the impressions from the original magnetic resonance (MR) imaging reports with the preoperative clinical impression and postoperative pathological diagnoses. The most commonly occurring masses were ganglia, lipomas, and giant cell tumors of tendon sheaths. MR imaging suggested the correct diagnosis in 16 of the 20 cases, whereas the clinical impression was correct in 10 instances. Confident preoperative diagnosis may be made with MR imaging due to the characteristic appearances of many benign soft tissue tumors.

Key words: Soft tissue tumors – Magnetic resonance imaging – Wrist

Evaluation of soft tissue masses is the most common indication for magnetic resonance (MR) evaluation of the wrist at our institution. While the usefulness of MR imaging for identifying the presence and extent of soft tissue tumors is widely accepted, controversy does remain in the literature regarding the ability of MR imaging to distinguish between benign and malignant lesions [1–3]. Numerous criteria, including margin definition, invasion of adjacent structures, and signal intensity, have been investigated with varying success [1–3], but the most useful finding is the fact that many benign soft tissue tumors have characteristic appearance which allow confident preoperative diagnosis [1, 4].

Materials and methods

The wrists of 20 patients with soft tissue masses were recently studied on a General Electric 1.5-T superconducting magnet (GE Medical Systems, Milwaukee, Wisconsin), using a variety of small extremity surface coils. Depending on the site of the mass, the field of view ranged from 8 to 12 cm. Pulse sequences included multiecho spin echo, fast spin echo, gradient recalled echo, and fat suppressed sequences.

Patients were positioned supine with the affected hand placed in pronation at the side. Axial plane sectioning provided the best anatomic delineation of the mass relative to adjacent structures. The coronal and sagittal planes permitted larger fields of view, depicting the extent of the mass.

The impressions from the original MR reports were compared with the preoperative clinical impressions and the postoperative histologic diagnosis.

Correspondence to: Hollis G. Potter, M.D., Department of Radiology, The Hospital for Special Surgery, 535 East 70th St., New York, NY 10021, USA

Results

The results are summarized in Table 1.

Discussion

The most commonly discovered mass was a ganglion cyst, which is a small fibrous walled mass containing clear mucinous fluid. It is common in the hands and feet and usually arises from joints, tendons, or tendon sheaths, especially on the extensor surface. Those cases which demonstrate a characteristic location and transillumination on physical examination may not warrant such an advanced imaging technique as MR. On MR imaging a ganglion cyst shows as a well-defined homogeneous mass with a signal intensity approximately equal to that of muscle on T1-weighted images (T1WI) and markedly increased signal intensity on T2-weighted images (T2WI) [5, 6] (Fig. 1). Occasionally, however, hemorrhage, trauma, or infection may cause an atypical appearance, making diagnosis difficult and requiring excisional biopsy (Figs. 2, 3).

A lipoma is an encapsulated mass composed of mature adipocytes. It is a soft tumor and may have an irregular contour if compressed between adjacent structures, but nevertheless remains well defined. The key diagnosis is the fact that it equals the signal intensity of subcuta-

Table 1. Summary of findings in 20 cases of soft tissue masses of the hand and wrist

Case no.	Gender	Patient age (years)	Site of mass	Clinical diagnosis	MR diagnosis	Pathologic diagnosis
1	F	65	Volar & ulnar aspect of wrist	GCT/ganglion	GCT of tendon sheath	GCT of tendon sheath
2	M	27	Volar & ulnar aspect of wrist	Solid ST mass	GCT of tendon sheath	GCT of tendon sheath
3	F	53	Volar aspect of wrist	Lipoma	Lipoma	Lipoma
4	F	41	Hypothenar eminence	Lipoma	Nonagressive fatty tumor	Lipoma
5	M	48	Extensor surface of wrist	Solid ST Mass	Atypical ganglion	Fibrous & mucoid tissue
6	M	35	Dorsum of wrist	Ganglion	Ganglion	Ganglion
7	F	61	First MCP joint	Chondrosarcoma	Synovial chondromatosis or soft tissue chondroma	Synovial chondromatosis
8	F	32	Ulnar side of wrist	Neurofibroma	Neurofibroma	Schwannoma
9	M	74	Palmar surface of hand	Solid ST mass	Atypical ganglion	Benign sweat gland tumor
10	F	4	Dorsum of wrist	Solid ST mass	Fibroma	Anomalous muscle
11	M	31	Forearm and hand	Hemangioma	Hemangioma	Hemangioma
12	M	4	3rd middle phalanx	ST mass	Fibromatosis	Lymphangioma
13	F	10	Volar wrist	ST mass	Fibrolipomatous hamartoma	Fibrolipomatous hamartoma
14	F	40	Palm between 4th & 5th metacarpal	Nerve sheath tumor	Focal fibroma	Dupuytren's contracture
15	F	33	Adjacent to first proximal phalanx	ST mass	Fibromatosis fat necrosis	Scar tissue with focal
16	M	51	Dorsal wrist	Cystic ST mass	Ganglion	Ganglion
17	F	40	Scapholunate joint	Cystic ST mass	Ganglion	Ganglion
18	M	34	Dorsal metacarpals	Cystic ST mass	Ganglion	Ganglion
19	M	28	Dorsal radio-Ulnar joint	Cystic ST mass	Ganglion	Ganglion
20	M	47	Dorsal metacarpals	Cystic ST mass	Ganglion	Ganglion

GCT, giant cell Tumor; ST, soft tissue; MCP, metacarpophalangeal

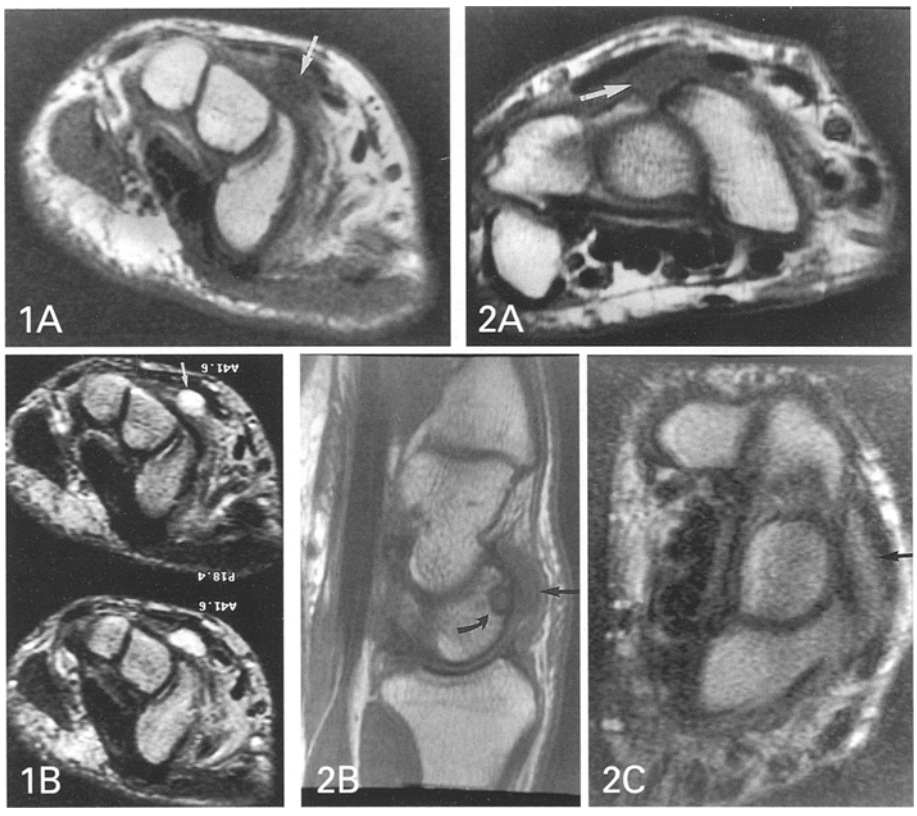

Fig. 1 A, B. Ganglion cyst. **A** Axial T1-weighted image (T1WI; TR/TE 500/16). There is a low signal intensity mass on the dorsum of the wrist (*arrow*), deep to the extensor tendons. **B** Axial T2-weighted image (T2WI; TR/TE 2100/80). The mass displays homogeneous high signal intensity and is sharply circumscribed

Fig. 2 A–C. Atypical ganglion cyst. **A** Axial T1WI (TR/TE 500/17). A poorly defined mass (*arrow*) is present on the dorsum of the wrist, deep to the extensor tendons and dorsal to the scapholunate joint. The signal is isointense to muscle. **B** Sagittal T1WI (TR/TE 500/17). The mass (*straight arrow*) overlies the dorsal surface of the lunate. A cyst is also present within the lunate (*curved arrow*), probably reflecting an intraosseus component. **C** Axial T2WI (TR/TE 2000/80). There is minimal increased signal intensity within the mass (*arrow*). While the location is suggestive of a ganglion, the indistinct borders and heterogeneity of the signal are atypical. Histological examination showed mucoid material and fibrous scar tissue.

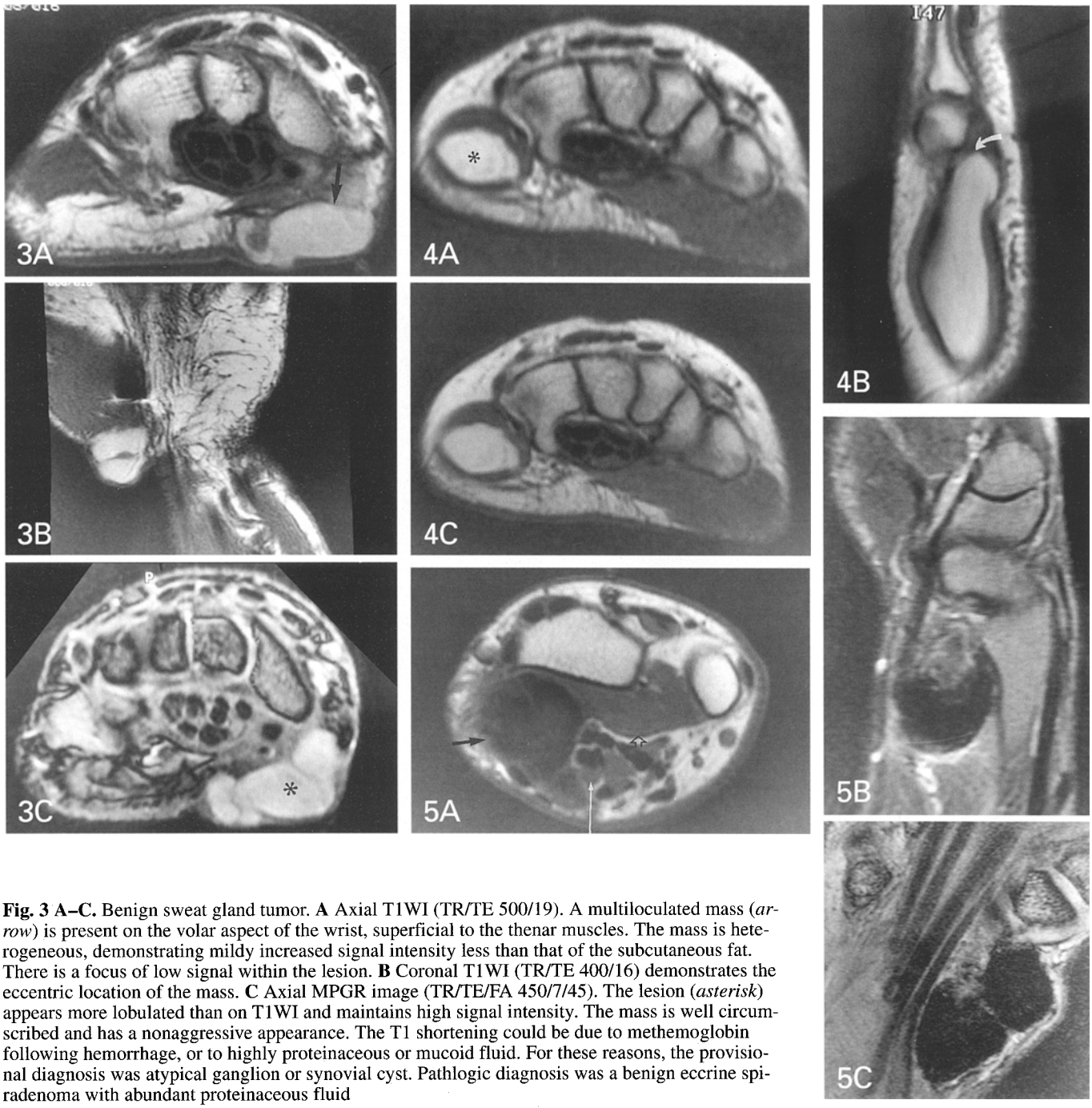

Fig. 3 A–C. Benign sweat gland tumor. **A** Axial T1WI (TR/TE 500/19). A multiloculated mass (*arrow*) is present on the volar aspect of the wrist, superficial to the thenar muscles. The mass is heterogeneous, demonstrating mildy increased signal intensity less than that of the subcutaneous fat. There is a focus of low signal within the lesion. **B** Coronal T1WI (TR/TE 400/16) demonstrates the eccentric location of the mass. **C** Axial MPGR image (TR/TE/FA 450/7/45). The lesion (*asterisk*) appears more lobulated than on T1WI and maintains high signal intensity. The mass is well circumscribed and has a nonaggressive appearance. The T1 shortening could be due to methemoglobin following hemorrhage, or to highly proteinaceous or mucoid fluid. For these reasons, the provisional diagnosis was atypical ganglion or synovial cyst. Pathlogic diagnosis was a benign eccrine spiradenoma with abundant proteinaceous fluid

Fig. 4 A–C. Intramuscular lipoma. **A** Axial T1WI (TR/TE 600/33). A well-circumscribed mass (*asterisk*) is present in the hypothenar muscles at the level of the hook of the hamate. The mass has the same signal intensity as the subcutaneous fat. **B** Sagittal T1WI (TR/TE 600/16) demonstrates the longitudinal extent of the lesion (*curved arrow*). **C** Axial T2WI (TR/TE 2500/70). The signal intensity is less than that on T1WI, and is equal to that of the subcutaneous fat

Fig. 5 A–C. Pigmented villonodular synovitis. **A** Axial T1WI (TR/TE 400/18). There is a low- to intermediate-signal-intensity mass (*black arrow*) on the radial side of the distal forearm, superficial to the pronator quadratus muscle (*open arrow*). The flexor digitorum tendons and muscles and median nerve (*white arrow*) are displaced ulnarly and are not encased. **B** Sagittal T2WI (TR/TE 2000/65) with fat suppression. The mass has low signal intensity. **C** Coronal MPGR (TR/TE/FA 250/15/45). The signal intensity of the lobulated mass is markedly decreased. The presence of low signal on all pulse sequences, especially on the gradient echo, is due to the paramagnetic dephasing effect of hemosidering, thus suggesting the diagnosis of pigmented villonodular synovitis

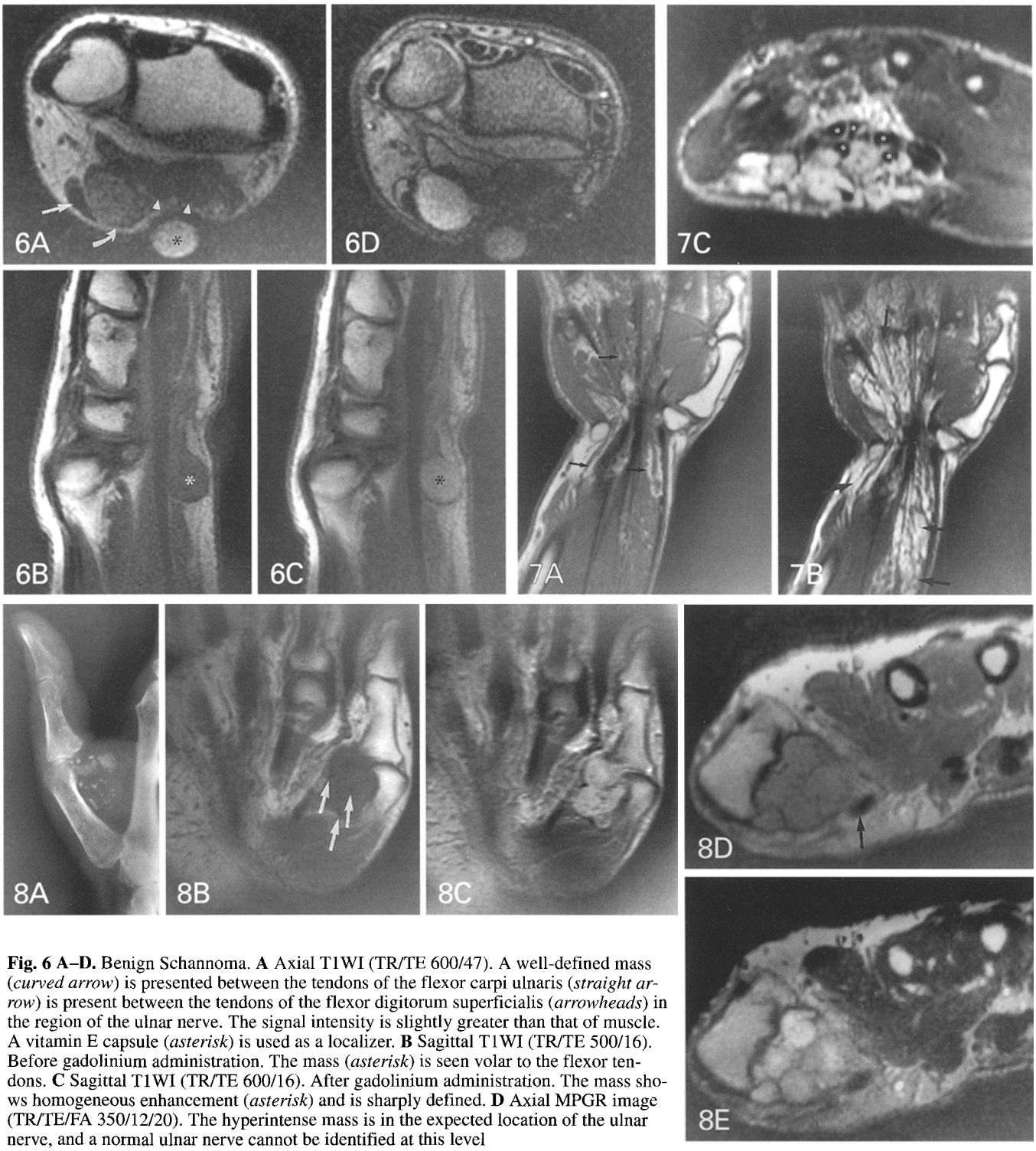

Fig. 6 A–D. Benign Schannoma. **A** Axial T1WI (TR/TE 600/47). A well-defined mass (*curved arrow*) is presented between the tendons of the flexor carpi ulnaris (*straight arrow*) is present between the tendons of the flexor digitorum superficialis (*arrowheads*) in the region of the ulnar nerve. The signal intensity is slightly greater than that of muscle. A vitamin E capsule (*asterisk*) is used as a localizer. **B** Sagittal T1WI (TR/TE 500/16). Before gadolinium administration. The mass (*asterisk*) is seen volar to the flexor tendons. **C** Sagittal T1WI (TR/TE 600/16). After gadolinium administration. The mass shows homogeneous enhancement (*asterisk*) and is sharply defined. **D** Axial MPGR image (TR/TE/FA 350/12/20). The hyperintense mass is in the expected location of the ulnar nerve, and a normal ulnar nerve cannot be identified at this level

Fig. 7A–C. Hemangioma. **A** Coronal T1WI (TR/TE 500/16). A large, poorly defined mass extends from the distal forearm into the hand. Areas of streaky or lacelike bright signal (*arrows*) within the mass represent areas of fat. **B** Coronal T2WI (TR/TE 2000/70). The mass displays heterogeneous bright signal and is quite extensive (*arrows*). **C** Axial T2WI (TR/TE 2000/80). The flexor digitorum tendons (*asterisks*) are encased by the lobulated and serpiginous mass

Fig. 8 A–E. Synovial osteochondromatosis. **A** Plain radiograph of the thumb. A soft tissue mass is present on the ulnar side of the first metacarpal bone and metacarpophalangeal joint. The mass has eroded portions of the first metacarpal and proximal phalanx, and has displaced the sesamoids. Numerous punctate calcifications are present in the mass. **B** Coronal T1WI(TR/TE 600/16). The mass is isointense to muscle, with punctate areas of signal void (*small arrows*) corresponding to the calcifications on the plain radiographs. **C** Coronal T2WI (TR/TE 2000/70). The lobulated nature of the mass is better appreciated. The mass is located at the ulnar aspect of the first metacarpal and metacarpophalangeal joint, and causes benign erosion of the metacarpal, without evidence of invasion, periosteal reaction, or marrow edema. **D** Axial first echo, fast spin echo sequence (TR/TE 3000/23). The borders of the mass are well delineated and the benign erosion of the metacarpal is seen again. There is ulnar and volar displacement of the flexor pollicis longus tendon (*arrow*). **E** Axial second echo, fast spin echo sequence (TR/TE 3000/115). The mass is lobulated and has heterogeneous high signal intensity, suggestive of a chondroid lesion

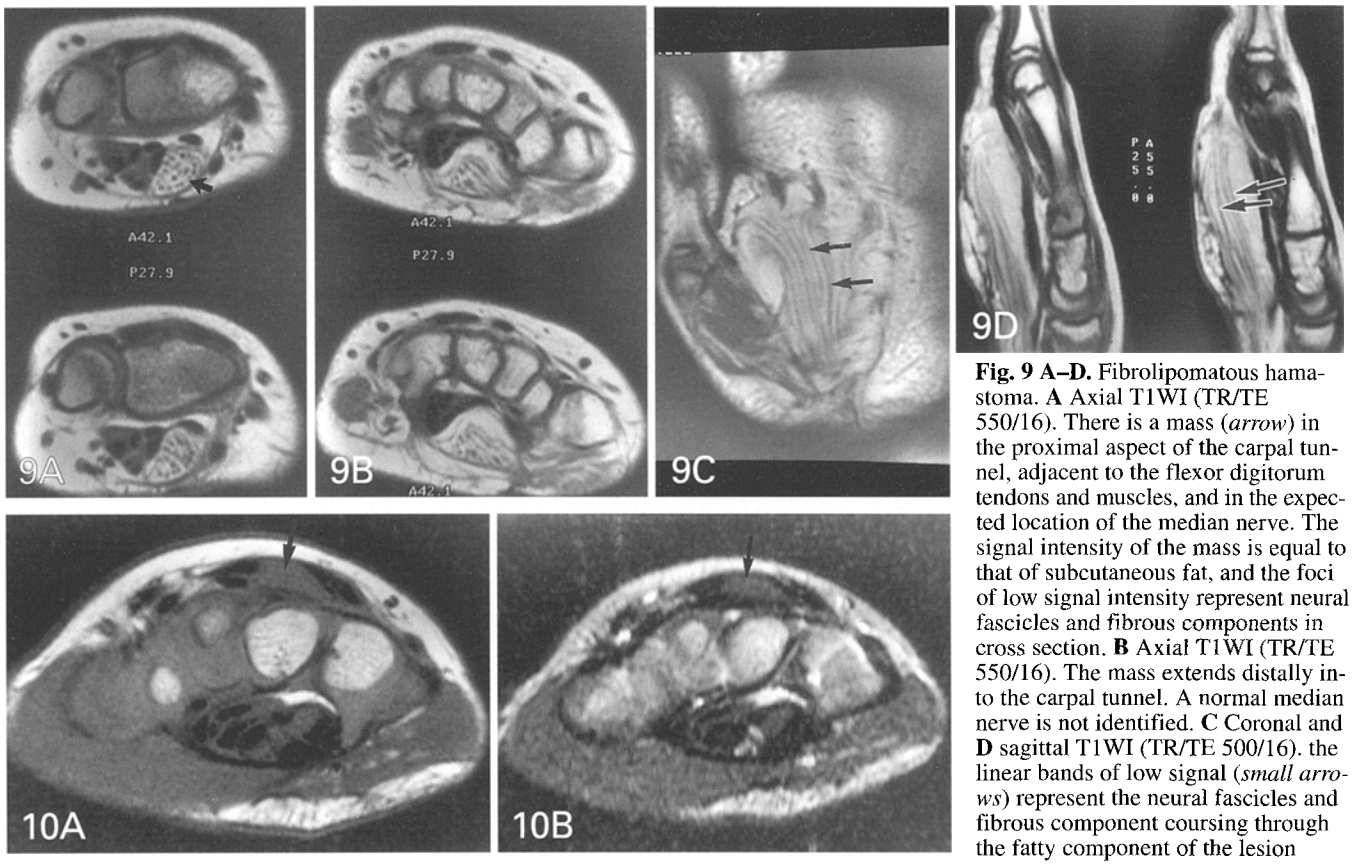

Fig. 9 A–D. Fibrolipomatous hamastoma. **A** Axial T1WI (TR/TE 550/16). There is a mass (*arrow*) in the proximal aspect of the carpal tunnel, adjacent to the flexor digitorum tendons and muscles, and in the expected location of the median nerve. The signal intensity of the mass is equal to that of subcutaneous fat, and the foci of low signal intensity represent neural fascicles and fibrous components in cross section. **B** Axial T1WI (TR/TE 550/16). The mass extends distally into the carpal tunnel. A normal median nerve is not identified. **C** Coronal and **D** sagittal T1WI (TR/TE 500/16). the linear bands of low signal (*small arrows*) represent the neural fascicles and fibrous component coursing through the fatty component of the lesion

Fig. 10 A, B. Anomalous muscles. **A** Axial T1WI (TR/TE 500/17). A mass (*arrow*) is present on the dorsum of the hand, between and deep to the extensor tendons. The signal intensity, and appearance of the mass are similar to those of muscle. **B** Axial T2WI (TR/TE 2000/80). The dorsal (*arrow*) mass displays the same signal intensity and appearance as muscle on all pulse sequences. The mass was excised and proved indeed to be anomalous skeletal muscle

neous fat on all pulse sequences [7] (Fig. 4). Low-signal-intensity fibrous septa are often present [7]. Occasionally, a well-differentiated lipoblastic liposarcoma may have a similar appearance, thus making differentiation difficult [1]. Frequency-selective fat suppressed or short TI inversion recovery (STIR) sequences may aid in the diagnosis of these lesions.

Pigmented villonodular synovitis is a monoarticular process which commonly occurs in the digits of the hands. The process may also occur extra-articularly, and is then called a giant cell tumor of tendon sheath. Histologically, it is composed of stromal cells, fibrous tissue, giant cells, and hemosiderin due to repeated hemorrhage. Typically, the tumor has low signal intensity on all pulse sequences due to the paramagnetic effect of hemosiderin (Fig. 5). This effect predominates on long TR/TE sequences, as hemosiderin acts primarily as a T2 signal dephaser. In addition, the tumor may display mild heterogeneity and a low-intensity-signal rim [6]. Less commonly, tumors may fail to demonstrate a focal hemosidering effect.

Benign tumors of peripheral nerves include neurofibroma and neurilemoma (benign schwannoma). On T1WI, they may have isointense of slightly greater signal intensity than adjacent muscle, and may have a homo- or heterogeneous texture [1, 3, 8]. On T2WI, they have brighter signal than muscle, but can still vary in homogeneity [1, 8]. They tend to be well defined on both pulse sequences, and their presence in the expected location of a nerve should suggest the diagnosis (Fig. 6), although the differentiation of benign and malignant types can be difficult [1].

A hemangioma is a benign vascular mass with variable amounts of nonvascular elements, of which fat usually predominates. The size of the tumor vessels determines whether the hemangioma is "capillary" or "cavernous." On T1WI the mass is generally isointense to muscle, with varying amounts of linear, lacelike, or coarse bright signal due to fat. It displays a heterogeneous bright signal on T2WI secondary to a high free water content within the pooled blood of the larger vessels, with a linear or lacelike area of low signal due to fibrous or muscular tissue (Fig. 7). Oval signal voids, representing phleboliths, may occasionally be seen [9].

Synovial chondromatosis is a condition in which there is cartilaginous metaplasia of the synovium, resulting in the formation of foci of hyaline cartilage. These cartilaginous areas may remain attached to the synovium, or may break free and become loose bodies within the joint. Mineralization of the metaplastic cartilage occurs in approximately 60%–70% of cases [10], and has a fairly typical appearance on plain films (Fig. 8 a). While the

diagnosis can usually be made from the conventional radiographs, MR imaging is useful for presurgical planning to determine the extent of the process and to determine the integrity and possible involvement of adjacent structures, such as collateral ligaments and tendons. On T2WI and gradient echo images, metaplastic cartilage has lobulated high signal intensity with signal voids due to foci of mineralization (Fig. 8 B–E).

A rare but distinctive-appearing tumor is the fibrolipomatous hamartoma, also known as a neural fibrolipoma. It usually presents in childhood or young adulthood as a slowly growing mass on the volar aspect of the hand or wrist. It almost always arises from the median nerve [11], and may give rise to symptoms of pain, paresthesia, or decreased sensation. In approximately one-third of cases there is associated macrodystrophia lipomatosa of the digits [7]. Pathologically, the tumor consists of infiltration of the nerve by fibrous and fatty elements, the relative amounts of which can vary. MR imaging shows serpiginous or circular low signal structures on both T1WI and T2WI representing the fibrous component, surrounded by various amounts of fat [7] (Fig. 9).

Lastly, anomalously placed muscle can present as pseudomasses on the plam or dorsum of the hand or as unsuspected causes of nerve entrapment. In particular, compression of the median nerve in the carpal tunnel by an accessory flexor digitorum superficialis or palmaris longus has been reported [12]. An anomalous muscle may be diagnosed on MR imaging by virtue of its nonaggressive appearance and signal characteristics, which are isointense to skeletal muscle on all pulse sequences (Fig. 10).

In conclusion, MR imaging may provide invaluable information regarding the delineation and differentiation of various soft tissue masses of the wrist and hand. In many instances a specific diagnosis can be made based on typical signal characteristics. Due to the variable appearance of several of these tumors, however, biopsy will occasionally be needed to exclude a more aggressive process.

References

1. Hermann G, Abdelwahab IF, Miller TT, Klein MJ, Lewis MM. Tumour and tumour-like conditions of the soft tissue:magnetic resonance imaging features differentiating benign from malignant masses. Br J Radiol 1992; 65: 14–20.
2. Berquist TH, Ehman RL, King BF, Hodgman CG, Ilstrup DM. Value of MR imaging in differentiating benign from malignant soft-tissue masses: study of 95 lesions. AJR 1990; 155: 1251–1255.
3. Kransdorf MJ, Jelinek JS, Moser RP Jr, et al. Soft-tissue masses: diagnosis using MR imaging. AJR 1989; 153: 541–547.
4. Jelinek JS, Kransdorf MJ. MR imaging of soft-tissue masses. AJR 1990; 155: 423–424
5. Binkovitz LA, Berquist TH, McLeod RA. Masses of the hand and wrist: detection and characterization with MR imaging. AJR 1990; 154: 323–326.
6. Wetzel LH, Levine E. Soft-tissue tumors of the foot: value of MR imaging for specific diagnosis. AJR 1990; 155: 1025–1030.
7. Kransdorf MJ, Moser RP Jr, Meis JM, Meyer CA. Fat-containing soft-tissue masses of the extremities. Radiographics 1991; 11: 81–106.
8. Petasnick JP, Turner DA, Charters JR, Gitelis S, Zacharias CE. Soft tissue masses of the locomotor system: comparison of MR imaging with CT. Radiology 1986; 160: 125–133.
9. Buetow PC, Kransdorf MJ, Moser RP Jr, Jelinek JS, Berrey BH. Radiologic appearance of intramuscular hemangioma with emphasis on MR imaging. AJR 1990; 154: 563–567.
10. Kaye JJ. Tumors in and around joints. In: Resnick D, Pettersson H, eds. Skeletal Radiology. London: Merit Communications, 1992.
11. Walker CW, Adams BD, Barnes CL, Roloson GJ, FitzRandolph RL. Case report 667: Fibrolipomatous hamartoma of the median nerve. Skeletal Radiol 1991; 20: 237–239.
12. Coenen L, Biltjes I. Pseudotumor of the palm due to an anomalous flexor digitorum superficialis muscle belly. J Hand Surg 1991; 16A:1046–1051.